Investigation of Halo Formation in Continuous Beams using Weighted Polynomial Expansions and Perturbational Analysis*

Christopher K. Allen, LANL, Los Alamos, New Mexico; ckallen@lanl.gov

Abstract

We consider halo formation in continuous beams oscillating at natural modes by inspecting particle trajectories. Trajectory equations containing field nonlinearities are derived from a weighted polynomial expansion. We then use perturbational techniques to further analyze particle motion.

1. INTRODUCTION

For continuous beams with elliptical symmetry, there are two natural oscillation modes: the symmetric, or even mode, and the anti-symmetric, or odd, mode. Halo formation is triggered by parametric resonances between the betatron motion of the particles and the natural modes of the collective beam [3]. The electric fields provided the coupling between the motions.

In the laboratory frame, the equations of motion for the x coordinate of a particle are

$$x'' + k_0^2(s)x = K\frac{2\pi\varepsilon_0}{\lambda}E_x(x,y,X,Y;s) \quad (1)$$

where k_0 is the focusing constant, λ is the line charge density, the generalized beam perveance K is

$$K \equiv \frac{qI}{2\pi\varepsilon_0}\frac{1}{mc^3\beta^3\gamma^3}, \quad (2)$$

I is the beam current, ε_0 is the permittivity of free space, β is normalized velocity, γ is the relativistic factor, and E_x is the self electric-field component. From these exact equations we shall derive trajectory equations which include the third order nonlinearities of the self-fields.

2. WEIGHTED FIELD EXPANSION

Here we assume that the self-field E_x may be represented with a polynomial expansion in the Cartesian coordinate variable x. Considering only the x-axis dynamics we have

$$E_x(x) \approx a_0 + a_1x + a_2x^2 + a_3x^3 + a_4x^4 + a_5x^5 + \ldots, \quad (3)$$

where the a_n are typically functions of the bunch envelopes. We are unlikely to find a polynomial expansion that closely approximates the true fields over the entire beam region. However, it is possible to find one that represents the bunch fields in an averaged sense. Letting $\langle\cdot,\cdot\rangle$ be a *weighted* inner product, this criterion translates into the following equation for coefficients a_n:

$$\begin{pmatrix} \langle 1,1\rangle & \langle 1,x\rangle & \langle 1,x^2\rangle & \langle 1,x^3\rangle \\ \langle x,1\rangle & \langle x,x\rangle & \langle x,x^2\rangle & \langle x,x^3\rangle \\ \langle x^2,1\rangle & \langle x^2,x\rangle & \langle x^2,x^2\rangle & \langle x^2,x^3\rangle \\ \langle x^3,1\rangle & \langle x^3,x\rangle & \langle x^3,x^2\rangle & \langle x^3,x^3\rangle \end{pmatrix}\begin{pmatrix} a_0 \\ a_1 \\ a_2 \\ a_3 \end{pmatrix} = \begin{pmatrix} \langle E_x,1\rangle \\ \langle E_x,x\rangle \\ \langle E_x,x^2\rangle \\ \langle E_x,x^3\rangle \end{pmatrix}. \quad (4)$$

The above matrix is the *Gram matrix* for the polynomial basis. The right-hand side represents the field projection onto the space of polynomials. We choose the weighting factor as the particle distribution itself. Regions of high density contribute proportionally more toward the expansion coefficients. This inner product is defined as

$$\langle u,v\rangle \equiv \frac{1}{qN}\int_{-\infty}^{+\infty}\int_{-\infty}^{+\infty} u(x,y)v(x,y)\,\rho(x,y)\,dxdy, \quad (5)$$

where q is the unit charge and N is the number of particles per cross-section. The inner product also generates the moment operator $\langle\cdot\rangle = \langle\cdot,1\rangle$. Thus, the Gram matrix is composed of the x plane moments $\langle x^n\rangle$ while the right-hand side of Eq. (4) contains the field moments $\langle x^nE_x\rangle$.

2.1 Computation of Electric Field Moments

It is possible to compute the field moments explicitly for beams having elliptical symmetry in configuration space. The self electric field of such a beam [2] is given by

$$E_x(x,y) = x\frac{qXY}{2\varepsilon_0}\int_0^\infty \frac{f[\frac{x^2}{t+X^2}+\frac{y^2}{t+Y^2}]}{(t+X^2)^{3/2}(t+Y^2)^{1/2}}dt, \quad (6)$$

where $f(\cdot)$ represents the profile of the distribution and X, Y represent the x, y envelopes of the equivalent uniform beam. To specify $\langle x^n\rangle$ and $\langle x^nE_x\rangle$ it is first convenient to introduce definitions involving the function f. We have

$$g(r) \equiv \int_r^\infty f(s)ds, \quad F_n \equiv \int_0^\infty s^n f(s)ds, \quad G_0 \equiv \int_0^\infty g^2(r)dr. \quad (7)$$

Now the first six nonzero spatial moments are

$$\langle 1\rangle = 1, \quad \langle x^2\rangle = \frac{X^2}{2}\frac{F_1}{F_0}, \quad \langle x^4\rangle = \frac{3X^4}{8}\frac{F_2}{F_0}, \quad \langle x^6\rangle = \frac{5X^6}{16}\frac{F_3}{F_0}. \quad (8)$$

Using Eq. (6), the nonzero field moments are

$$\begin{aligned} \langle xE_x\rangle &= \frac{\lambda}{4\pi\varepsilon_0}\frac{X}{X+Y}, \\ \langle x^3E_x\rangle &= \frac{\lambda}{4\pi\varepsilon_0}\left[\frac{F_1}{F_0}\frac{X^3}{X+Y} + \left(\frac{F_1}{F_0} - \frac{3}{2}\frac{G_0}{F_0^2}\right)\frac{X^3Y}{(X+Y)^2}\right]. \end{aligned} \quad (9)$$

* Work supported by the US Department of Energy

2.2 Cubic Expansion of Self-Fields

To expand the self-fields out to third order we must keep terms up to a_3. The resulting particle trajectory equation is

$$x'' + k_0^2 x - \frac{2K}{X(X+Y)}\left[\Gamma_1 + \Gamma_2 \frac{Y}{X+Y}\right]x + \frac{2K}{X^3(X+Y)}\left[\Gamma_3 + \Gamma_4 \frac{Y}{X+Y}\right]x^3 = 0 . \tag{10}$$

where the Γ_i are functions of the distribution. Thus, we have separated the effects of the distribution from the motion of the envelopes X and Y. The values of Γ_i are

$$\Gamma_1 \equiv \frac{5F_0F_3 - 6F_1F_2}{10F_1F_3 - 9F_2^2}, \qquad \Gamma_3 \equiv \frac{6F_0F_2 - 8F_1^2}{10F_1F_3 - 9F_2^2},$$
$$\Gamma_2 \equiv \frac{9G_0F_2/F_0 - 6F_1F_2}{10F_1F_3 - 9F_2^2}, \qquad \Gamma_4 \equiv \frac{12F_1G_0/F_0 - 8F_1^2}{10F_1F_3 - 9F_2^2}. \tag{11}$$

Table *1* lists the Γ_i for several different distributions.

Table 1 : distribution expansion coefficients

Distrib.	$f(x)$	Γ_1	Γ_2	Γ_3	Γ_4
Uniform	C $x \le 1$	1	0	0	0
Parabolic	$C(1-x)$ $x \le 1$	2	-2/5	4/3	-16/15
Gaussian	Ce^{-2x}	3/2	-1/4	2/3	-1/3
Hollow	Cxe^{-2x}	8/13	-3/52	4/39	-2/39

2.3 Examples

To compare with previously published work on halo formation [3], we normalize the above equations. We shall also assume even mode excitation of the envelopes, so that $X(s)$=$Y(s)$=$R(s)$. The normalizations are

$$\tau = k_0 s \qquad r(\tau) = R(k_0 s)/R_0 \qquad \xi'(\tau) = \frac{x'(s)}{k_0 R_0}$$
$$k_E = k_0\sqrt{2+2\eta^2} \qquad \xi(\tau) = x(k_0 s)/R_0 \tag{12}$$

where η is the tune depression and R_0 is the equilibrium radius. The resulting unit-less trajectory equations are

$$\xi'' + \xi - \frac{1-\eta^2}{r^2}\left(\Gamma_1 + \frac{\Gamma_2}{2}\right)\xi + \frac{1-\eta^2}{r^4}\left(\Gamma_3 + \frac{\Gamma_4}{2}\right)\xi^3 = 0, \tag{13}$$

Figure 1 shows surface of section plots for the normalized trajectory equations at η=0.5 and a Gaussian distribution. We took $r(\tau)$=1+$\varepsilon\cos\kappa\tau$ where κ=k_E/k_0. In each plot twenty trajectories where started from evenly spaced positions on the x-axis. There is clearly a two-to-one resonance condition with the beam envelopes, identifiable from the (two) period-two fixed points seen along the x-axis. By increasing the mismatch parameter ε, the stable islands shrink and the velocity of the trajectories increases. The noticeable difference between these results and that of the particle-core model is that the fixed points are located at smaller values.

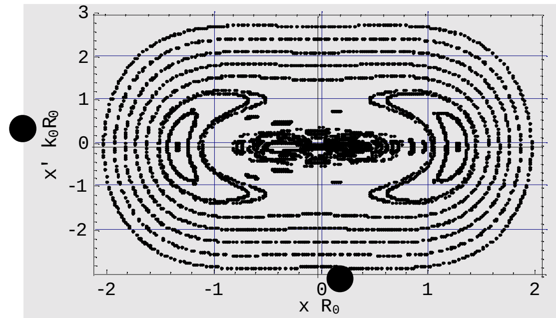

a) phase portrait for ε=0.25

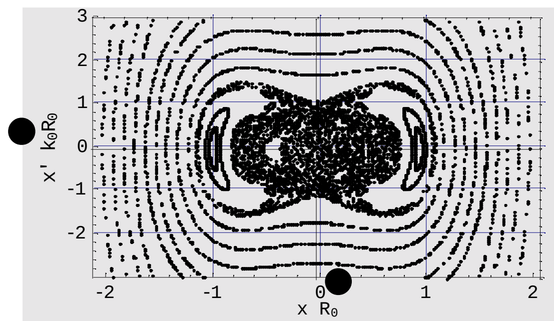

b) phase portrait for ε=0.50

Figure 1: stroboscopic plots for trajectory equations

3. PERTURBATION ANALYSIS

Here we assume that the transverse beam envelopes $X(s)$ and $Y(s)$ (of the equivalent uniform beam) perform small oscillations about a nominal value R_0. The wave numbers of these oscillations are k_E and k_O for the even and odd modes, respectively. Thus,

$$X(s) = R_0 + \varepsilon R_0 \cos k_{E,O} s,$$
$$Y(s) = R_0 \pm \varepsilon R_0 \cos k_{E,O} s, \tag{14}$$

where ε is the (small) mismatch parameter. Using a multi-scale perturbation analysis about ε, we find a first-order approximation to the trajectory solutions [1]. Situations near parametric resonance are considered by employing a (small) “detuning” parameter δ defined below. We find

$$x(s) \approx \sqrt{\varepsilon}\, a(\varepsilon s)\cos[ks + \phi(\varepsilon s)], \tag{15}$$

where the functions $a(t)$ and $\phi(t)$ satisfy

$$a'(t) = \frac{C_{E,O}}{4k} a(t)\sin(2\delta t + 2\phi),$$
$$\phi'(t) = \frac{3C_3}{8k} a^2(t) + \frac{C_{E,O}}{4k}\cos(2\delta t + 2\phi), \tag{16}$$

with the following definitions:

$$k = k_0\eta \equiv k_0\sqrt{1 - \frac{K}{k_0^2 R_0^2}\frac{(2\Gamma_1 + \Gamma_2)}{2}}\ , \tag{17}$$

$$C_E = \frac{K}{R_0^2}(2\Gamma_1 + \Gamma_2) = 2(k_0^2 - k^2),$$

(18) $$C_O = \frac{K}{R_0^2}(\Gamma_1 + \Gamma_2) = 2(k_0^2 - k^2)\frac{\Gamma_1 + \Gamma_2}{2\Gamma_1 + \Gamma_2},$$

$$C_3 = \frac{K}{2R_0^4}(2\Gamma_3 + \Gamma_4) = \frac{k_0^2 - k^2}{R_0^2}\frac{2\Gamma_3 + \Gamma_4}{2\Gamma_1 + \Gamma_2},$$

(19) $$\delta \equiv (k - \frac{1}{2}k_{E,O})/\varepsilon .$$

Note that the definition of η here is different then in Section 2. Also, the above is valid only when $\delta \ll k$. This system admits the solution

(20) $$a(t) = A \equiv \sqrt{\frac{2C_{E,O}}{3C_3} - \frac{8k}{3C_3}\delta},$$
$$\phi(t) = -\delta t - \frac{\pi}{2},$$

which corresponds to the period-two fixed points seen in the stroboscopic plots. Near this stable solution, the system performs linear oscillations with wave number κ

(21) $$\kappa \equiv \sqrt{\frac{3C_3 C_{E,O}}{8k^2}}A .$$

The resulting linearized approximation is

(22) $$x(s) \approx \sqrt{\varepsilon}[A + A_0 \cos \varepsilon\kappa s] \cdot \cos\left(\frac{1}{2}k_{E,O}s + A_0\sqrt{\frac{3C_3}{2C_{E,O}}}\sin\varepsilon\kappa s - \frac{\pi}{2}\right),$$

where A_0 is an arbitrary constant.

3.1 Analysis

The period-two fixed point is found by taking A_0=0. The magnitude of the fixed point x_{fp}, for $\delta \approx 0$, is approximately

(23) $$x_{fp} \approx \frac{2}{\sqrt{3}}\sqrt{\varepsilon}R_0\sqrt{\frac{2\Gamma_1 + \Gamma_2}{2\Gamma_3 + \Gamma_4}} .$$

The distance down the channel needed to develop halo, say l_h, can be inferred from κ. A complete amplitude oscillation yields $\kappa l_h = 2\pi$. Letting δ=0, l_h should scale as

(24) $$l_h \sim \frac{1}{\varepsilon}\frac{2\pi}{k_0}\frac{\eta}{1-\eta^2} .$$

3.2 Examples

To examine the accuracy of the perturbation equations we compare them with the full equations using the following parameters for the even mode: Γ_i=Gaussian, ε=0.25, R_0=1.8 mm, k_0=3.2 rad/m, η=0.9 (K=4.59×10^{-9}). The trajectories were started at x=0.1 mm, x'=0 mrad. In Eqs. (16), we took δ=0 for worst case and set k_E=2k in the full equations. Figure 2 shows numeric solutions of the perturbation equations and the full trajectory equations. The amplitude of the approximate solution is larger, probably due to the fact that δ=0. Here we get l_h=37 m. If the initial conditions are started closer to the fixed point, the amplitude period is approximately l_h. The location of the fixed point is x_{fp}=1.72 mm. Solving the full equations, we find that the true value is 1.5 mm.

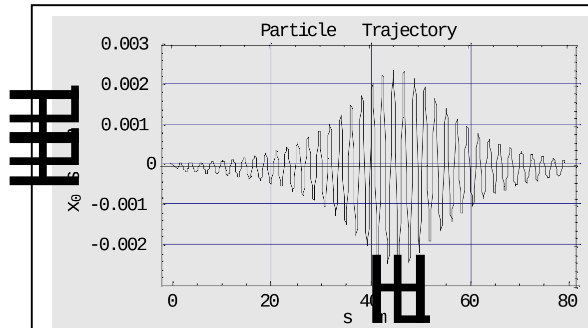

a) perturbation equation solution

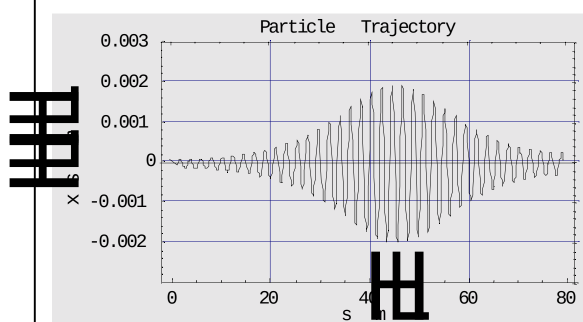

b) full trajectory equation solution

Figure 2: comparison of nonlinear trajectories

4. CONCLUSION

The availability of ordinary differential equations describing nonlinear particle trajectories in a mismatched beam simplifies the study of many aspects of halo formation. Further, it is possible to use the trajectory equations in conjunction with the envelope equations to obtain more consistent computer solutions. Another avenue of further study is beam behavior in presence of alternating gradient (AG) focusing.

REFERENCES

[1] M.H. Holmes, *Introduction to Perturbation Methods* (Springer-Verlag, New York, 1995) pp. 287-291.

[2] O.D. Kellogg, Foundations of Potential Theory (Dover, 1953) pp. 192-194.

[3] T.P. Wangler, K.R. Crandall, R. Ryne and T.S. Wang, "Particle-core model for transverse dynamics of beam halo", *Phys. Rev. Special Topics, Accel. and Beams*, Vol. 1, No. 084201 (1998).